Hypoxic microenvironment as a crucial factor triggering events leading to rupture of intracranial aneurysm

Isao Ono
National Cerebral and Cardiovascular Center
Tomomichi Kayahara
National Cerebral and Cardiovascular Center
Akitsugu Kawashima
Tokyo Women's Medical University Yachiyo Medical Center
Akihiro Okada
National Cerebral and Cardiovascular Center
Susumu Miyamoto
Kyoto University Graduate School of Medicine
Hiroharu Kataoka
National Cerebral and Cardiovascular Center
Hiroki Kurita
Saitama Medical University International Medical Center
Akira Ishii
Kyoto University Graduate School of Medicine
Tomohiro Aoki (tomoaoki@ncvc.go.jp)
National Cerebral and Cardiovascular Center

Research Article

Keywords: intracranial aneurysm, subarachnoid hemorrhage, vasa vasorum, neovessel, hypoxia, VEGF

Posted Date: May 11th, 2022

DOI: https://doi.org/10.21203/rs.3.rs-1520573/v2

Abstract

Subarachnoid hemorrhage being the rupture of intracranial aneurysm (IA) as a major cause has a high mortality rate. It is thus mandatory for social health to clarify mechanisms regulating rupture of IAs and to develop a novel therapeutic strategy. Recently, the formation of vasa vasorum in lesions presumably for inflammatory cells to infiltrate in lesions has been clarified as a potential histopathological alternation leading to rupture. We clarified the origin of this structure as arteries on brain surface and the presence of hypoxic microenvironment mainly at the adventitia of intracranial arteries where IA is induced. The production of vascular endothelial growth factor (VEGF) not only from cultured macrophages in such a hypoxic condition but also at rupture-prone IA lesions induced in a rat model was clarified. We further found the accumulation of VEGF in human unruptured IA lesions, supporting the production of VEGF *in situ*. Finally, we confirmed the VEGF-dependent migration of neovessels into subarachnoid space from arteries on brain surface. Because of the lack of vasa vasorum and being surrounded by cerebrospinal fluid space, the formation of hypoxic microenvironment becomes a character of intracranial arteries and inflammatory responses could further facilitate such a condition. Additionally, the attachment of IA to brain surface might be an important factor for the migration of vasa vasorum from arteries on brain surface. The findings have revealed the potential role of hypoxic microenvironment as a potential machinery triggering rupture of IAs via providing root for inflammatory cells to infiltrate into lesions and exacerbate inflammation.

Background

Intracranial aneurysm (IA), a regional bulging of intracranial arteries, can develop subarachnoid hemorrhage (SAH) after rupture and becomes a major cause of it [1, 2]. Nowadays, more and more cases with unruptured IAs is found in clinical settings, meaning the presence of a chance to apply medical interventions to prevent rupture. Because of poor outcome once after the onset of SAH in spite of the technical advancement of the treatment and the medical care [1, 2], the development of a novel therapeutic strategy to prevent rupture of IA lesions is mandatory for public health. For this purpose, precise molecular mechanisms underlying the process leading to rupture of the lesions should be clarified to identify therapeutic targets.

Through a series of studies mainly using animal models of IAs, we and others have successfully defined IA as a chronic inflammatory disease affecting intracranial arteries mainly at bifurcation sites [3-17]. Here, we have recently proposed the potential mechanisms; the formation of vasa vasorum provides the root for inflammatory cells, mainly macrophages and neutrophils, to facilitate the infiltration in lesions and triggers the exacerbation of inflammation *in situ* leading to rupture of IA lesions [10, 18]. In addition, the contribution of neutrophils to the onset of SAH is also supported by the experiment in which GM-CSF, Granulocyte Macrophage colony-stimulating Factor, facilitated rupture of IAs via the increase in infiltrating neutrophils [10]. Thereby, the underlying machinery to induce vasa vasorum at the adventitia could be a therapeutic target to prevent rupture of IAs. Here, hypoxia and the hypoxia-induced expression of angiogenic factor, most typically vascular endothelial growth factor (VEGF), are well-established and

potent inducer of angiogenesis [19-21], the formation of vasa vasorum in case of IAs [18]. Because intracranial arteries histologically lack vasa vasorum [22], the adventitia of intracranial arteries consists of the hypoxic microenvironment in nature and the past reports have indeed demonstrated the oxygen partial pressure in the adventitia as approximate 40 mmHg [23-25]. We therefore examined the presence of hypoxia in rupture-prone or ruptured lesions and the expression of angiogenic factors in lesions.

Methods

IA models of rats and histological analysis of induced IA

10-week-old female Sprague–Dawley rats were purchased from Japan SLC (Slc:SD, n=20, Shizuoka, Japan). Animals were maintained on a light/dark cycle of 12 h/12 h, and had a free access to chow and water. To induce IAs [10, 18, 26], rats were subjected to the bilateral ovariectomy, the ligation of the left carotid artery, the right external carotid artery and the right pterygopalatine artery, and systemic hypertension achieved by the combination of a high salt diet and the ligation of the left renal artery under general anesthesia by the inhalation of Isoflurane (induction; 5.0 %, maintenance; 1.5~2.0 %, #IYESC-0001, Pfizer Inc., New York, NY). Immediately after surgical manipulations, animals were fed the chow containing 8 % sodium chloride and 0.12 % 3-aminopropionitrile (#A0408, Tokyo Chemical Industry, Tokyo, Japan), an irreversible inhibitor of Lysyl Oxidase catalyzing the cross-linking of collagen and elastin. At 16 weeks after above surgical manipulations, animals were deeply anesthetized by the inhalation of Isoflurane (5.0 %, #IYESC-0001, Pfizer Inc.), and transcardially perfused with 4 % paraformaldehyde solution. The circle of Willis was then stripped from brain surface and an IA lesion induced at an anterior communicating artery or a posterior communicating artery was dissected.

Tissue transparency and immunohistochemistry

Tissue transparency was done using paraformaldehyde-fixed specimens and CUBIC-L and CUBIC-R solutions (#T3740 or #T3741, TCI chemicals, Tokyo, Japan) as manufacturer's instructions. Immunohistochemistry to visualize medial smooth muscle cells was done using a CUBIC-HV 3D Immunostaining Kit and mouse monoclonal anti-a-smooth muscle actin antibody conjugated with Cy3 (#C6198, clone 1A4, Sigma, St. Louis, MI) as manufacturer's instructions. The images were acquired by a confocal laser microscopy (FV3000, Olympus, Tokyo, Japan).

Immunohistochemistry

In specimens from animals, 5-μm-thick frozen sections were prepared from dissected IA lesions or anterior cerebral – olfactory artery bifurcations, aorta or liver prepared as described above. After blocking with 3 % donkey serum (#AB_2337258, Jackson ImmunoResearch), slices were incubated with primary antibodies followed by incubation with secondary antibodies conjugated with a fluorescence dye (Jackson ImmunoResearch). In some experiments, the primary antibody conjugated with a fluorescence dye was used. Finally, fluorescent images were acquired on a confocal fluorescence microscope system (FV3000, Olympus, Tokyo, Japan).

In specimens from human cases, dissected human specimen was fixed in formalin solution and embedded in paraffin. 4-μm-thick slices were then prepared for immunohistochemical analysis. After deparaffinization and blocking with 10 % donkey serum (Jackson ImmunoResearch), slices were incubated with primary antibodies followed by incubation with secondary antibodies conjugated with fluorescence dye (Jackson ImmunoResearch). Finally, fluorescent images were acquired on a confocal fluorescence microscope system (FV3000, Olympus).

The antibodies used were as follows; mouse monoclonal anti-a-smooth muscle actin antibody (#M0851, Dako, Agilent, Santa Clara, CA), mouse monoclonal anti-a-smooth muscle actin antibody conjugated with Cy3 (#C6198, Sigma), mouse monoclonal anti-CD68 antibody conjugated with Alexa Fluor 647 (#sc-20060AF647, Santa Cruz Biotechnology, Dallas, TX), mouse monoclonal anti-VEGF antibody (clone VG1, #NB100-664, Novus Biologicals, LLC, Centennial, CO), mouse monoclonal anti-Pimonidazole antibody (clone MAb1, #HP1-100, Hypoxyprobe, Inc., Burlington, MA) , Alexa Fluor 488-conjugated donkey anti-mouse IgG H&L antibody (#A21202, Thermo Fisher Scientific, Waltham, MA), Alexa Fluor 594-conjugated donkey anti-mouse IgG H&L antibody (#A21203, Thermo Fisher Scientific).

Detection of hypoxic cells and tissues *in vivo*

To detect hypoxic cells or tissues *in vivo*, Hypoxyprobe was used (Hypoxyprobe, Inc.). This probe is the derivative of Pimonidazole which binds to hypoxic cells and can be detected in immunohistochemistry using the specific antibody for Hypoxyprobe delivered from the company. 60 mg/kg of Hypoxyprobe was intraperitoneally injected in rats and after 165 min the specimens were harvested subjecting to immunohistochemistry as in the above section.

Induction of vasa vasorum from arteries at brain surface by VEGF

Burr hole was prepared in the skull of rats by high-speed drill system under general anesthesia as described above and the sheets for the slow-release of VEGF was placed on the brain surface (MedGel II from Nitta-gelatin (#PI9, Osaka Japan) and recombinant human VEGF (1 μg/head, #564-RV-010/CF, lot #CWC0620081) from R&D systems, Inc. (Minneapolis, MN) resolved in phosphate buffered saline containing 0.1% human serum albumin (#A1653-5G, lot #SLBG2676V, Sigma). The induction of vasa vasorum was then assessed by histological examination and by immunohistochemistry on 6^{th} day as described above.

Cell culture

RAW264.7 cell line, NIH3T3 cell line and U937 cell line were purchased from ATCC (#TIB-71 for RAW264.7, #CRL-1658 for NIH3T3, #CRL-1593.2 for U937, Manassas, VA). Cells were maintained in Dulbecco's Modified Eagle Medium (#044-29765, FUJIFILM Wako Chemicals, Osaka Japan) supplemented with 10 % fetal bovine serum (#FB-1365/500, lot#11953, biosera, Nuaille, France) (RAW264.7 cells and NIH3T3 cells) or RPMI-1640 (#189-02025, FUJIFILM Wako Chemicals) with 10 % fetal bovine serum (#FB-1365/500, lot#11953, biosera) (U937 cells).

Loading hypoxia on cultured cells

To load hypoxia, cells were incubated in a hypoxia chamber system (0.5 % or 5 %, #BIONIX-2, SUGIYAMA-GEN CO., LTD., Tokyo, Japan) for 8 h.

RNA purification and quantitative real time (RT)-PCR analysis

Total RNA was purified from treated cells and reverse-transcribed using a RNeasy Mini Kit (#74106, QIAGEN, Hilden, Germany) and a High-capacity cDNA Reverse Transcription Kit (#4368813, Life Technologies Corporation, Carlsbad, CA), according to the manufacturers' instructions. For quantification of gene expression, quantitative RT-PCR was performed on a LightCycler 480 (Roche, Indianapolis, IN) with a TB Green Premix Ex Taq II (#RR820, TAKARA BIO INC., Shiga, Japan). Expression of *Actb* (a gene coding β-actin) was used as internal controls. For quantitation, the second derivative maximum method was used for determining the crossing point.

Primer sets used are listed as follows: 5'-ACGACCAGAGGCATACAGGGA-3' and 5'-CCCTAAGGCCAACCGTGAAA-3' for *Actb*; forward 5'-GGTCTGTTGGGAGTGGTATCC-3' and reverse 5'-TTCCTCTCTGCAAGAGACTTCC-3' for *Il6*; forward 5'-AAAGGGAGCTCCTTAACATGC-3' and reverse 5'-CTTCCTGGGAAACAACAGTGG-3' for *Il1b*; forward 5'-AATGATGTGTACGGCTTCAGG-3' and reverse 5'-CTGTACAAGCAGTGGCAAAGG-3' for *Ptgs2* (cyclooxygenase-2 (COX-2)); forward 5'-GCACAGACCTCTCTCTTGAGC-3' and reverse 5'-ACCTGCTGCTGCTACTCATTCACC-3' for *Ccl2* (also known as MCP-1; monocyte chemoattractant protein-1); forward 5'-GCAGTGCATACCACTTCAACC-3' and reverse 5'-CTGATGGTCAAGATCCAGAGG-3' for *Nos2*; forward 5'- AAAGCAGGTCAGTCACTTTGC-3' and reverse 5'-TCACTCCCTCAAATCACTTCG-3' for *Vegf* exon 1; forward 5'- GGAGAGATGAGCTTCCTACAGC-3' and reverse 5'-GGATTTCTTGCGCTTTCG-3' for *Vegf* exon 4-6; forward 5'- TCACATCTGCAAGTACGTTCG-3' and reverse 5'- ACTGTGAGCCTTGTTCAGAGC-3' for *Vegf* exon 7-8; 5'-ACCTCTCTTCCCACAGAAAGC-3' and 5'-CTTAGGCTCAGGCCATTATGC-3' for *Areg* (Amphiregulin); 5'-GCACGAAGATCAAGAACAACG-3' and 5'-AGGAGCCTCTAGCTTCACACC-3' for *Ang* (Angiogenin); 5'-ACAACAACCACCACAATCACC-3' and 5'-GGTATGTGCCGACATTACAGG-3' for *Angpt1* (Angiopoietin-1); 5'-CAGTCTCTGAAGGTGGTTTGC-3' and 5'-CAGCATGACCTAATGGAGACC-3' for *Angpt2* (Angiopoietin-2); 5'-TTGGTGGACAGTGAGTTCTCC-3' and 5'-AACCAGACCAAAGCTCAGACC-3' for *Angpt4* (Angiopoietin-4); 5'-ACAGCTCAACTCAGTGCTTCC-3' and 5'-GCCTATAGGGTTACGGTTTGG-3' for *Cnn1* (Calponin 1); 5'-GTAAGATTTGGCGAACAGACG-3' and 5'-TAATGTCCGAAGTGGTCATCG-3' for *Dll4* (Delta like canonical Notch ligand 4); 5'-GGATGGAGGTTAATCCTGACC-3' and 5'-GGCACAGTTTGTCTTCAATGG-3' for *Egf* (Epidermal growth factor); 5'-CCAGAGGGAGCTCTACAAAGG-3' and 5'-AGATCTTTCCAGGAAGCAAGG-3' for *Eng* (Endoglin); 5'-AGGACGATGTAGCTGTTGTGG-3' and 5'-ATGGCGAACTGAAACTACTGG-3' for *Col18a1* (Collagen, type XVIII, alpha 1); 5'-CAGTACAGGCATGTTCCAAGC-3' and 5'-CGATGAGCAGTGTTTGAAAGC-3' for *Fgf7* (Fibroblast growth factor 7); 5'-CTTTCTGGCAAGAACTTGTGC-3' and 5'-CACAAGCAATCCAGAGGTACG-3' for *Hgf* (Hepatocyte growth factor); 5'-CAGCTTTGGTTACACAATCAGC-3' and 5'-GAAGCTTTCAGTGGGTTAGGG-3' for *Igfbp1* (Insulin-like growth factor binding protein 1); 5'-TGCTGTTCATTGACCTTCTCC-3' and 5'-AGGTTGCAGACAGTGATGACG-3' for *Igfbp2* (Insulin-like growth

factor binding protein 2); 5'-AGAAGTTCTGGGTGTCTGTGC-3' and 5'-ATTCCAAGTTCCATCCACTCC-3' for *Igfbp3* (Insulin-like growth factor binding protein 3); 5'-GTTCGGCTCAAACTTCTCTCC-3' and 5'-CTGAGATGAGACCCTGTGACC-3' for *Ccn3* (Cellular communication network factor 3); 5'-ACTTCTCTTCCTGCGAATGG-3' and 5'-GAAGTCAGATCCACAGCATCC-3' for *Pdgfa* (Platelet derived growth factor, alpha); 5'-GGCAAGTTGGCCATATTTAGG-3' and 5'-TATATTCCACTCCAGCCAAGC-3' for *Pdgfb* (Platelet derived growth factor, B polypeptide); 5'-TGTCCACTGCTCACATACAGC-3' and 5'-GGCATTCAGAAGCAGAGAGG-3' for *Serpine1* (Serine (or cysteine) peptidase inhibitor, clade E, member 1); 5'-TAGTCTAGCGGGAAGGTGAGG-3' and 5'-CAGCAAGATTACTGGCAAACC-3' for *Serpinf1* (Serine (or cysteine) peptidase inhibitor, clade F, member 1); 5'-ATGTATGGGCAGTTGTCTTGG-3' and 5'-TGACCAGAGAGATACGGATGG-3' for *Thbs2* (Thrombospondin 2); 5'- CATACTCCTGCTTGCTGATCC-3' and 5'-GATGCAGAAGGAGATCACTGC-3' for *ACTB*; 5'-ACACCCTCTATCACTGGCATCC-3' and 5'-AACATTCCTACCACCAGCAACC-3' for *PTGS2*; 5'-TCAGCAATGAGTGACAGTTGG-3' and 5'-ATAGGCTGTTCCCATGTAGCC-3' for *TNF*; 5'-CATTTGTGGTTGGGTCAGG-3' and 5'-AGTGAGGAACAAGCCAGAGC-3' for *IL6*; 5'-ATTCAGCACAGGACTCTCTGG-3' and 5'-CAAGCTGGAATTTGAGTCTGC-3' for *IL1B*; 5'-AGCTTCTTTGGGACACTTGC-3' and 5'-ATAGCAGCCACCTTCATTCC-3' for *CCL2*; 5'-GACCTGATGTTGCCATTGTTGG-3' and 5'-TACCAACTGACGGGAGATGAGC-3' for *NOS2*

Concentration of VEGF in the supernatant from hypoxia-loaded RAW264.7 cells

The supernatant from hypoxia-loaded RAW264.7 (0.5 %, 0~24 h) was collected subjecting to ELISA (#RSD-MMV00-1, R&D Systems) to examine the concentration of VEGF according to the manufacture's indications.

Statistics

Data are shown as Mean ± S.E.M. Differences between the 2 groups were examined using a non-parametric Mann-Whitney test. Differences more than 3 groups were examined using a Kruskal-Wallis test followed by a Steel test. A p value smaller than 0.05 was defined as statistically significant.

Results

The identification of the origin of vasa vasorum as arteries at brain surface

Because intracranial arteries histologically lack vasa vasorum [22] (Fig. 1), we examined where vasa vasorum came from by the combined technique of immunohistochemistry to visualize vascular smooth muscle cells with tissue transparency. In ruptured IA walls, arteries located on brain surface run toward the dome of IAs especially around the site of rupture where signals for the marker for vascular smooth muscle cells, a-smooth muscle actin, were absent (Fig. 2a). The presence of vasa vasorum with medial smooth muscle cells around the site of rupture in IAs was also confirmed in slices (Fig. 2b).

The presence of hypoxic microenvironment at the adventitia of intracranial arteries

We first hypothesized that the adventitia of intracranial arteries was under the hypoxic condition because of the lack of vasa vasorum [22 and the low oxygen partial pressure in CSF [23-25. To assess the hypothesis, Hypoxyprobe, the derivative of Pimonidazole which binds to hypoxic cells, was administered to rats subjecting to the immunohistochemistry using the specific antibody to examine the presence of this probe in intracranial arterial walls, liver used as a positive control [27]or aorta. As a result, the signals for Hypoxyprobe were observed in cells located at the adventitia of intracranial arterial walls (Fig. 3a) and the cells located around the central vein in liver served as a positive control (Fig. 3b), supporting above hypothesis. Intriguingly, the positive signals for Hypoxyprobe could be only sparsely observed in aorta in which vasa vasorum was present (Fig. 3c), indicating the originality of intracranial arterial walls.

Induction of VEGF and other angiogenic factors in cultured macrophages or fibroblasts under hypoxic condition

As intracranial arteries histologically lack vasa vasorum [22], the adventitia of intracranial arteries consists of the hypoxic microenvironment, approximate 40 mmHg [23-25] which corresponds to 5 % oxygen. We thereby first examined the effect of the physiological hypoxic condition at the adventitia (5 % oxygen) on the expression of a major angiogenic factor, VEGF, in cultured macrophages, RAW264.7 cells. We then found that hypoxia at the physiological level in the adventitia induced expression of *Vegf* in RAW264.7 cells (Fig. 4a). We next loaded cells on much lower oxygen partial pressure (0.5 %), the pathological hypoxia which may be loaded in inflammatory microenvironment of the lesions where many inflammatory cells accumulated and many types of cells activated. Such a pathological hypoxic condition also induced the expression of *Vegf* as well not only in cultured macrophages, RAW264.7 cells, but also in cultured fibroblasts, NIH3T3 cells (Fig. 4a). In cultured fibroblasts, the alternative splicing form of VEGF lacking exon 6 might be produced. The secretion of VEGF protein from hypoxia-treated RAW264.7 cells was also confirmed by ELISA (Fig. 4b). The expression of angiogenesis-related factors other than *Vegf* in hypoxia-stimulated RAW264.7 cells was also examined. Only a small number of factors was induced under the hypoxic condition, indicating the central role of VEGF in macrophages under hypoxic condition (Fig. 4c).

In addition, hypoxia loaded on cells induced expressions of some pro-inflammatory genes in various types of cells including *Ptgs2* (a gene for COX-2) or *Ccl2* (Fig. 4d). The induced expression of COX-2 might exacerbate inflammation via forming the positive feedback loop, COX-2-Prostaglandin E_2-Prostaglandin E receptor subtype 2 (EP2)-NF-kB [3], and the secretion of Ccl2 forms the auto-amplification of macrophages [3], indicating the further amplification of chronic inflammation *in situ*.

The expression of VEGF in IA walls induced in rats

We next examined whether VEGF was indeed expressed in rupture-prone IAs, where vasa vasorum was induced [18, in immunohistochemistry. The signals for VEGF were then detected in IA lesions in immunohistochemistry. Because the most signals for VEGF were well co-localized with those for the macrophage marker, CD68, the major source to produce VEGF in rupture-prone IA lesions was

macrophages infiltrating in the lesions (Fig. 5). The induction of VEGF from infiltrating macrophages was supported in above *in vitro* experiment.

The expression of VEGF in human IA walls

To evaluate the clinical relevance of the results from animal experiments, we immunostained slices from human IA lesions to examine the expression of VEGF. The signals for VEGF in immunohistochemistry could be observed and be widely distributed in all the specimens from human cases with unruptured IAs (Fig. 6), suggesting the sustained production of VEGF to some extent during IA progression.

The above results combined together might indicate the accumulation of VEGF from infiltrating macrophages in addition to sustained production during the process leading to rupture of IAs. The results that in human IA lesions VEGF constitutively expressed might, furthermore, indicate the necessity of the close of the dome of IAs to the arteries on brain surface and the collapse of CSF space and the disruption of arachnoid which could be physical barrier to prevent the migration of neovessels.

The VEGF-dependent induction of vasa vasorum from arteries on brain surface

To corroborate the induction of vasa vasorum from arteries on brain surface by VEGF, the effect of recombinant VEGF slowly-released into the subarachnoid space on the migration of neovessels was examined *in vivo*. The sheet for slow-release containing recombinant VEGF or vehicle was placed on brain surface (Fig. 7a) and the induction of neovessels in the subarachnoid space was histologically assessed. As a result, the presence of small arteries with medial smooth muscle cell layer could be observed only in the subarachnoid space of the VEGF-treated side (Fig. 7b-d), confirming the VEGF-dependent neovessel formation from arteries on brain surface.

Discussion

The major limitation of the present study is the lack of experimental evidence that VEGF in IA lesions indeed plays a crucial role to the rupture of IAs through inducing vasa vasorum formation at the adventitia. For example, the genetic deletion of VEGF in rats or the intrathecal administration of anti-VEGF antibody to neutralize VEGF from macrophages may become potential experiments. However, both experiments are challenging. We have used the rat model of IAs in a series of studies and the establishment of a rat line deficient in *Vegf* specifically in macrophages, which is necessary for experiments because the genetic deletion of VEGF in a whole body is lethal [28], is technically difficult. Furthermore, it takes long, several months, to assess the effect of a drug or an antibody on the onset of SAH in rats, making the repeat intrathecal administration of anti-VEGF antibody being necessary.

Considered with the devastating outcome once after the onset of SAH by the rupture of IAs [1, 2] and the nature as an asymptomatic lesion before rupture, machineries underlying the rupture can be a major therapeutic target. Through our previous studies [10, 18], the formation of vasa vasorum at the adventitia, which provides the root for inflammatory cells to infiltrate in the lesions, is presumably the crucial step to

drive IAs toward rupture. Thereby, the mechanism promoting the formation of vasa vasorum could be a therapeutic target. Because one of the most potent inducers for neovascularization is hypoxia and hypoxia-induced VEGF functions as a crucial mediator in this step [19–21], we in the present study examined the potential contribution of hypoxia and hypoxia-induced VEGF expression in IA lesions. We have then clarified the expression of VEGF at the prospective site where IA ruptures. Experiments using Hypoxyprobe have revealed the hypoxic microenvironment at the adventitia of intracranial arteries. Considered with the potent induction of VEGF among angiogenesis-related factors mainly from macrophages, the accumulation of this type of cells may increase the concentration of angiogenic factors *in situ* to induce the migration of intracranial arteries leading to the formation of vasa vasorum. Because VEGF can also increase permeability of endothelial barrier [29–31], the increase in VEGF *in situ* may further facilitate the accumulation of macrophages exacerbating the macrophage-mediated inflammation. Here, VEGF expression is transcriptionally induced by the activation of NF-κB [32–35] and we have clarified the activation of this transcription factor in macrophages as a major regulator of inflammatory responses in lesions [3, 6]. Thereby, macrophage-mediated inflammatory environment *in situ* presumably further accelerates the secretion of VEGF from macrophages and accumulation of this angiogenic factor in tissues. In addition to the triggering or the exacerbation of inflammatory responses, macrophages again plays the crucial role in the formation of vasa vasorum through VEGF production. Intriguingly, hypoxia induces the expression of pro-inflammatory genes which significantly contribute to the pathogenesis of IAs [3, 4, 8, 9, 12, 36–39]. Among these factors, COX-2 forms the positive feedback loop consisting of COX-2-Prostaglandin E_2-EP2-NF-κB, which we have identified as a crucial one to regulate chronic inflammation in lesions [3, 39], and CCL2 forms the auto-amplification loop among macrophages to provide sites for macrophage-mediated chronic inflammation to maintain inflammatory responses [3, 4, 39]. The induction of COX-2 and CCL2 therefore results in the exacerbation of inflammatory responses presumably leading to excessive degeneration of arterial walls and to rupture of lesions. These results combined together suggest the multiple roles of hypoxia, one is to provide the root for inflammatory cells to effectively infiltrate via the formation of vasa vasorum and the other is the exacerbation of inflammation, in the process triggering rupture of IAs. In this sense, chronic inflammatory responses still function as a crucial machinery regulating the disease in addition to the role in the initiation and growth of the lesions [3, 6, 12]. Such a concept is in line with the clinical evidence that drugs with anti-inflammatory effect like statins or aspirins exert the suppressive effect on the onset of SAH in the case-control studies [40–45].

In the present study, we have observed the origin of vasa vasorum as arteries attached to brain surface. Intracranial arteries, where IAs are formed, pass through the subarachnoid space and are anchored by arachnoid in places in CSF space. The adventitia in intracranial arteries thus primarily contact with CSF. Not only the distance between the adventitia of the lesions and arteries on brain surface but also CSF space therefore become the physical barrier to prevent the elongation of neovessels to the adventitia from the brain surface. The close of the dome of IAs to the arteries at brain surface and/or the collapse of CSF space might be a necessary factor to the formation of vasa vasorum, leading to rupture of the lesions. The sustained expression of VEGF in unruptured IA lesions presumably being in the hypoxic

condition in nature might support the above hypothesis. Here, it is well known that the larger size or the specific location of IAs significantly increases the risk of rupture of IA lesions [46, 47]. These two well-established risk factors can narrow the space to facilitate the formation of vasa vasorum at the adventitia.

Recently, the potential of vessel wall imaging by contrast-MRI as a diagnostic method to stratify dangerous IA lesions from many stable ones [48–52]. The precise mechanism of the enhancement in danger lesions, ruptured or growing ones, is not revealed until now. However, because the arterial wall in vasa vasorum is often leaky and also the blood flow is slow, the enhancement in this imaging method may reflect the presence of vasa vasorum which we have identified as the potential machinery to trigger rupture of IAs.

Conclusions

Considered with the poor outcome of SAH due to rupture of IAs, the development of a novel therapeutic strategy to prevent rupture based on the pathogenesis is mandatory for social health. Based on the recent experiment findings that vasa vasorum formation is the potential machinery to trigger rupture of IAs via facilitating the infiltration of inflammatory cells to exacerbate chronic inflammation *in situ*. We thus in the present study examined mechanisms regulating the formation of vasa vasorum and then found the presence of hypoxic microenvironment at the adventitia of intracranial arteries where IA is induced. Among angiogenic factors, the production of VEGF in the lesions including infiltrating macrophages and the potential contribution of this angiogenic factor to the induction of vasa vasorum *in vivo* were revealed. Here, because intracranial arteries histologically lack vasa vasorum and are surrounded by CSF space, the formation of the hypoxic microenvironment could be a character of intracranial arteries and inflammatory responses there might further facilitate such a condition to induce vasa vasorum. In addition, the enlargement of the lesions and the disruption of physical barrier like arachnoid could lead to the migration of vasa vasorum from arteries at brain surface. The findings from the present study have thus revealed the potential role of hypoxic microenvironment and hypoxia-induced VEGF production as a machinery triggering the rupture of IAs via providing root for inflammatory cells to exacerbate inflammation in the microenvironment of the lesions.

Abbreviations

COX-2; cyclooxygenase-2

CSF; cerebrospinal fluid

EP2; Prostaglandin E receptor subtype 2

IA; intracranial aneurysm

RT-PCR; real time-PCR

SAH; subarachnoid hemorrhage

SMA; a-smooth muscle actin

VEGF; vascular endothelial growth factor

Declarations

Ethics approval and consent to participate

Human unruptured IA samples and control arterial walls (superficial temporal artery) were obtained during neck clipping with the written informed consent. The use of human samples in the present study was approved by the Ethics Committee at Kyoto University Graduate School and Faculty of Medicine (Approval Number #E2540 and #R0601), National Cerebral and Cardiovascular Center (Approval Number #M29-050, #R21012), and Tokyo Women's Medical University Yachiyo Medical Center (Approval Number #4106) where samples were prepared. Also, the written informed consent was obtained from each case.

All of the following experiments, including animal care and use, complied with the National Institute of Health's Guide for the Care and Use of Laboratory Animals and complied with the National Institute of Health's Guide for the Care and Use of Laboratory Animals and were approved by the Institutional Animal Care and Use Committee of National Cerebral and Cardiovascular Center (Approval Number; #20003, #21015, #22041). The present manuscript adheres to the ARRIVE (Animal Research: Reporting of In Vivo Experiments) guidelines for reporting animal experiments.

Consent for publication

Not applicable.

Availability of data and materials

The datasets used and/or analyzed during the current study are available from the corresponding author on reasonable request.

Competing interests

All the authors declare that they have no competing interests

Funding

This work was supported by the Japan Agency for Medical Research and Development (AMED) (grant number #JP21ek0210148, H.Kataoka), and by Grant-in-Aid for Scientific Research from The Ministry of Education, Culture, Sports, Science and Technology (grant number #20K09381, T.A., #20K09367, H.Kataoka, #21K16622, T.K.).

Author's contributions

T.K., H.Kataoka and T. A. got the grant. I.O., T.K., H.Kataoka and T. A. planned the experiments. A. K. acquired human specimen. I.O., T.K., A.O. and T. A. acquired the data. I.O., T.K., A.O. H.Kataoka. and T. A. interpreted the data. I.O., T.K. and T.A. wrote the manuscript. S.M., H.Kataoka, H.Kurita, A.I. and T. A. critically reviewed and modified the manuscript. All authors read and approved the final manuscript.

Acknowledgements

Not applicable.

References

1. van Gijn J, Kerr RS, Rinkel GJ. Subarachnoid haemorrhage. Lancet. Jan 27 2007;369(9558):306–318. https://doi.org/10.1016/S0140-6736(07)60153-6
2. Lawton MT, Vates GE. Subarachnoid Hemorrhage. *The New England journal of medicine.* Jul 20 2017;377(3):257–266. https://doi.10.1056/NEJMcp1605827
3. Aoki T, Frosen J, Fukuda M, et al. Prostaglandin E2-EP2-NF-kappaB signaling in macrophages as a potential therapeutic target for intracranial aneurysms. *Sci Signal.* Feb 7 2017;10(465). https://doi.10.1126/scisignal.aah6037
4. Aoki T, Kataoka H, Ishibashi R, Nozaki K, Egashira K, Hashimoto N. Impact of monocyte chemoattractant protein-1 deficiency on cerebral aneurysm formation. Stroke; a journal of cerebral circulation. Mar 2009;40(3):942–951. https://doi.org/10.1161/STROKEAHA.108.532556
5. Aoki T, Kataoka H, Morimoto M, Nozaki K, Hashimoto N. Macrophage-derived matrix metalloproteinase-2 and – 9 promote the progression of cerebral aneurysms in rats. Stroke; a journal of cerebral circulation. Jan 2007;38(1):162–169. https://doi.org/10.1161/01.STR.0000252129.18605.c8
6. Aoki T, Kataoka H, Shimamura M, et al. NF-kappaB is a key mediator of cerebral aneurysm formation. Circulation. Dec 11 2007;116(24):2830–2840. https://doi.org/10.1161/CIRCULATIONAHA.107.728303
7. Aoki T, Yamamoto K, Fukuda M, Shimogonya Y, Fukuda S, Narumiya S. Sustained expression of MCP-1 by low wall shear stress loading concomitant with turbulent flow on endothelial cells of intracranial aneurysm. *Acta neuropathologica communications.* May 9 2016;4(1):48. https://doi.10.1186/s40478-016-0318-3.
8. Frosen J, Cebral J, Robertson AM, Aoki T. Flow-induced, inflammation-mediated arterial wall remodeling in the formation and progression of intracranial aneurysms. Neurosurg Focus. Jul 1 2019;47(1):E21. https://doi.org/10.3171/2019.5.FOCUS19234
9. Kanematsu Y, Kanematsu M, Kurihara C, et al. Critical roles of macrophages in the formation of intracranial aneurysm. Stroke; a journal of cerebral circulation. Jan 2011;42(1):173–178. https://doi.org/10.1161/STROKEAHA.110.590976

10. Kushamae M, Miyata H, Shirai M, et al. Involvement of neutrophils in machineries underlying the rupture of intracranial aneurysms in rats. Sci Rep. Nov 17 2020;10(1):20004. https://doi.org/10.1038/s41598-020-74594-9
11. Oka M, Shimo S, Ohno N, et al. Dedifferentiation of smooth muscle cells in intracranial aneurysms and its potential contribution to the pathogenesis. Sci Rep. May 20 2020;10(1):8330. https://doi.org/10.1038/s41598-020-65361-x
12. Shimizu K, Kushamae M, Mizutani T, Aoki T. Intracranial Aneurysm as a Macrophage-mediated Inflammatory Disease. *Neurol Med Chir (Tokyo).* Apr 15 2019;59(4):126–132. https://doi.10.2176/nmc.st.2018-0326
13. Turjman AS, Turjman F, Edelman ER. Role of fluid dynamics and inflammation in intracranial aneurysm formation. *Circulation.* Jan 21 2014;129(3):373–382. https://doi.org/10.1161/CIRCULATIONAHA.113.001444
14. Frosen J, Piippo A, Paetau A, et al. Remodeling of saccular cerebral artery aneurysm wall is associated with rupture: histological analysis of 24 unruptured and 42 ruptured cases. Stroke; a journal of cerebral circulation. Oct 2004;35(10):2287–2293. https://doi.org/10.1161/01.STR.0000140636.30204.da
15. Chyatte D, Bruno G, Desai S, Todor DR. Inflammation and intracranial aneurysms. Neurosurgery. Nov 1999;45(5):1137–1146; discussion 1146 – 1137. https://doi.org/ 10.1097/00006123-199911000-00024
16. Hasan D, Hashimoto T, Kung D, Macdonald RL, Winn HR, Heistad D. Upregulation of cyclooxygenase-2 (COX-2) and microsomal prostaglandin E2 synthase-1 (mPGES-1) in wall of ruptured human cerebral aneurysms: preliminary results. Stroke; a journal of cerebral circulation. Jul 2012;43(7):1964–1967. https://doi.org/10.1161/STROKEAHA.112.655829
17. Hasan DM, Chalouhi N, Jabbour P, et al. Evidence that acetylsalicylic acid attenuates inflammation in the walls of human cerebral aneurysms: preliminary results. Journal of the American Heart Association. Feb 2013;2(1):e000019. https://doi.org/10.1161/JAHA.112.000019
18. Miyata H, Imai H, Koseki H, et al. Vasa vasorum formation is associated with rupture of intracranial aneurysms. Journal of neurosurgery. Aug 16 2019:1–11. https://doi.org/10.3171/2019.5.JNS19405
19. Ikeda H, Kakeya H. Targeting hypoxia-inducible factor 1 (HIF-1) signaling with natural products toward cancer chemotherapy. J Antibiot (Tokyo). Oct 2021;74(10):687–695.
20. Richard DE, Berra E, Pouyssegur J. Angiogenesis: how a tumor adapts to hypoxia. Biochemical and biophysical research communications. Dec 29 1999;266(3):718–722. https://doi.org/10.1006/bbrc.1999.1889
21. Rahimi N. The ubiquitin-proteasome system meets angiogenesis. Molecular cancer therapeutics. Mar 2012;11(3):538–548. https://doi.org/10.1158/1535-7163.MCT-11-0555
22. Clower BR, Sullivan DM, Smith RR. Intracranial vessels lack vasa vasorum. Journal of neurosurgery. Jul 1984;61(1):44–48. https://doi.org/10.3171/jns.1984.61.1.0044

23. Dunkin RS, Bondurant S. The determinants of cerebrospinal fluid Po2. The effects of oxygen and carbon dioxide breathing in patients with chronic lung disease. Ann Intern Med. Jan 1966;64(1):71–80. https://doi.org/10.7326/0003-4819-64-1-71
24. Rossanda M, Gordon E. The oxygen tension of cerebrospinal fluid in patients with brain lesions. Acta Anaesthesiol Scand. 1970;14(3):173–181. https://doi.org/10.1111/j.1399-6576.1970.tb00963.x
25. Zupping R. Cerebral acid-base and gas metabolism in brain injury. Journal of neurosurgery. Nov 1970;33(5):498–505. https://doi.org/10.3171/jns.1970.33.5.0498
26. Oka M, Ono I, Shimizu K, et al. The Bilateral Ovariectomy in a Female Animal Exacerbates the Pathogenesis of an Intracranial Aneurysm. Brain Sci. May 31 2020;10(6). https://doi.org/10.3390/brainsci10060335
27. Samoszuk MK, Walter J, Mechetner E. Improved immunohistochemical method for detecting hypoxia gradients in mouse tissues and tumors. J Histochem Cytochem. Jun 2004;52(6):837–839. https://doi.org/10.1369/jhc.4B6248.2004
28. Carmeliet P, Ferreira V, Breier G, et al. Abnormal blood vessel development and lethality in embryos lacking a single VEGF allele. Nature. Apr 4 1996;380(6573):435–439. https://doi.org/10.1038/380435a0
29. Aguilar-Cazares D, Chavez-Dominguez R, Carlos-Reyes A, Lopez-Camarillo C, Hernadez de la Cruz ON, Lopez-Gonzalez JS. Contribution of Angiogenesis to Inflammation and Cancer. Front Oncol. 2019;9:1399. https://doi.org/10.3389/fonc.2019.01399
30. Bates DO. Vascular endothelial growth factors and vascular permeability. Cardiovasc Res. Jul 15 2010;87(2):262–271. https://doi.org/10.1093/cvr/cvq105
31. Claesson-Welsh L, Dejana E, McDonald DM. Permeability of the Endothelial Barrier: Identifying and Reconciling Controversies. Trends Mol Med. Apr 2021;27(4):314–331. https://doi.org/10.1016/j.molmed.2020.11.006
32. Fu CY, Wang PC, Tsai HJ. Competitive binding between Seryl-tRNA synthetase/YY1 complex and NFKB1 at the distal segment results in differential regulation of human vegfa promoter activity during angiogenesis. Nucleic Acids Res. Mar 17 2017;45(5):2423–2437. https://doi.org/10.1093/nar/gkw1187
33. Walton CB, Matter ML. Chromatin Immunoprecipitation Assay: Examining the Interaction of NFkB with the VEGF Promoter. Methods Mol Biol. 2015;1332:75–87. https://doi.org/10.1007/978-1-4939-2917-7_6
34. Leychenko A, Konorev E, Jijiwa M, Matter ML. Stretch-induced hypertrophy activates NFkB-mediated VEGF secretion in adult cardiomyocytes. PloS one. 2011;6(12):e29055. https://doi.org/10.1371/journal.pone.0029055
35. Huang S, Robinson JB, Deguzman A, Bucana CD, Fidler IJ. Blockade of nuclear factor-kappaB signaling inhibits angiogenesis and tumorigenicity of human ovarian cancer cells by suppressing expression of vascular endothelial growth factor and interleukin 8. Cancer research. Oct 1 2000;60(19):5334–5339. http://cancerres.aacrjournals.org/content/60/19/5334

36. Aoki T, Nishimura M, Matsuoka T, et al. PGE(2) -EP(2) signalling in endothelium is activated by haemodynamic stress and induces cerebral aneurysm through an amplifying loop via NF-kappaB. British journal of pharmacology. Jul 2011;163(6):1237–1249. https://doi.org/10.1111/j.1476-5381.2011.01358.x
37. Fukuda S, Hashimoto N, Naritomi H, et al. Prevention of rat cerebral aneurysm formation by inhibition of nitric oxide synthase. Circulation. May 30 2000;101(21):2532–2538. https://doi.org/10.1161/01.CIR.101.21.2532
38. Sadamasa N, Nozaki K, Hashimoto N. Disruption of gene for inducible nitric oxide synthase reduces progression of cerebral aneurysms. Stroke; a journal of cerebral circulation. Dec 2003;34(12):2980–2984. https://doi.org/10.1161/01.STR.0000102556.55600.3B
39. Aoki T, Narumiya S. Prostaglandins and chronic inflammation. Trends in pharmacological sciences. Jun 2012;33(6):304–311. https://doi.org/10.1016/j.tips.2012.02.004
40. Yoshimura Y, Murakami Y, Saitoh M, et al. Statin use and risk of cerebral aneurysm rupture: a hospital-based case-control study in Japan. Journal of stroke and cerebrovascular diseases: the official journal of National Stroke Association. Feb 2014;23(2):343–348. https://doi.org/10.1016/j.jstrokecerebrovasdis.2013.04.022
41. Hasan DM, Mahaney KB, Brown RD, Jr., et al. Aspirin as a promising agent for decreasing incidence of cerebral aneurysm rupture. Stroke; a journal of cerebral circulation. Nov 2011;42(11):3156–3162. https://doi.org/10.1161/STROKEAHA.111.626762
42. Shimizu K, Imamura H, Tani S, et al. Candidate drugs for preventive treatment of unruptured intracranial aneurysms: A cross-sectional study. PloS one. 2021;16(2):e0246865. https://doi.org/10.1371/journal.pone.0246865
43. Can A, Castro VM, Dligach D, et al. Lipid-Lowering Agents and High HDL (High-Density Lipoprotein) Are Inversely Associated With Intracranial Aneurysm Rupture. Stroke; a journal of cerebral circulation. May 2018;49(5):1148–1154. https://doi.org/10.1161/STROKEAHA.117.019972
44. Can A, Rudy RF, Castro VM, et al. Association between aspirin dose and subarachnoid hemorrhage from saccular aneurysms: A case-control study. *Neurology.* Sep 18 2018;91(12):e1175-e1181. https://doi.org/10.1212/WNL.0000000000006200
45. Weng JC, Wang J, Du X, et al. Safety of Aspirin Use in Patients With Stroke and Small Unruptured Aneurysms. Neurology. Jan 5 2021;96(1):e19-e29. https://doi.org/10.1212/WNL.0000000000010997
46. Morita A, Kirino T, Hashi K, et al. The natural course of unruptured cerebral aneurysms in a Japanese cohort. *The New England journal of medicine.* Jun 28 2012;366(26):2474–2482. https://doi.10.1056/NEJMoa1113260
47. Greving JP, Wermer MJ, Brown RD, Jr., et al. Development of the PHASES score for prediction of risk of rupture of intracranial aneurysms: a pooled analysis of six prospective cohort studies. The Lancet Neurology. Jan 2014;13(1):59–66. https://doi.org/10.1016/S1474-4422(13)70263-1
48. Matsushige T, Shimonaga K, Mizoue T, et al. Lessons from Vessel Wall Imaging of Intracranial Aneurysms: New Era of Aneurysm Evaluation beyond Morphology. Neurol Med Chir (Tokyo). Nov 15

2019;59(11):407–414. https://doi.org/10.2176/nmc.ra.2019-0103

49. Edjlali M, Gentric JC, Regent-Rodriguez C, et al. Does aneurysmal wall enhancement on vessel wall MRI help to distinguish stable from unstable intracranial aneurysms? Stroke; a journal of cerebral circulation. Dec 2014;45(12):3704–3706. https://doi.org/10.1161/STROKEAHA.114.006626
50. Edjlali M, Guedon A, Ben Hassen W, et al. Circumferential Thick Enhancement at Vessel Wall MRI Has High Specificity for Intracranial Aneurysm Instability. Radiology. Oct 2018;289(1):181–187. https://doi.org/10.1148/radiol.2018172879
51. Hu P, Yang Q, Wang DD, Guan SC, Zhang HQ. Wall enhancement on high-resolution magnetic resonance imaging may predict an unsteady state of an intracranial saccular aneurysm. Neuroradiology. Oct 2016;58(10):979–985. https://doi.org/10.1007/s00234-016-1729-3
52. Wang GX, Wen L, Lei S, et al. Wall enhancement ratio and partial wall enhancement on MRI associated with the rupture of intracranial aneurysms. J Neurointerv Surg. Jun 2018;10(6):566–570. https://doi.org/10.1016/j.ejrad.2019.01.016

Figures

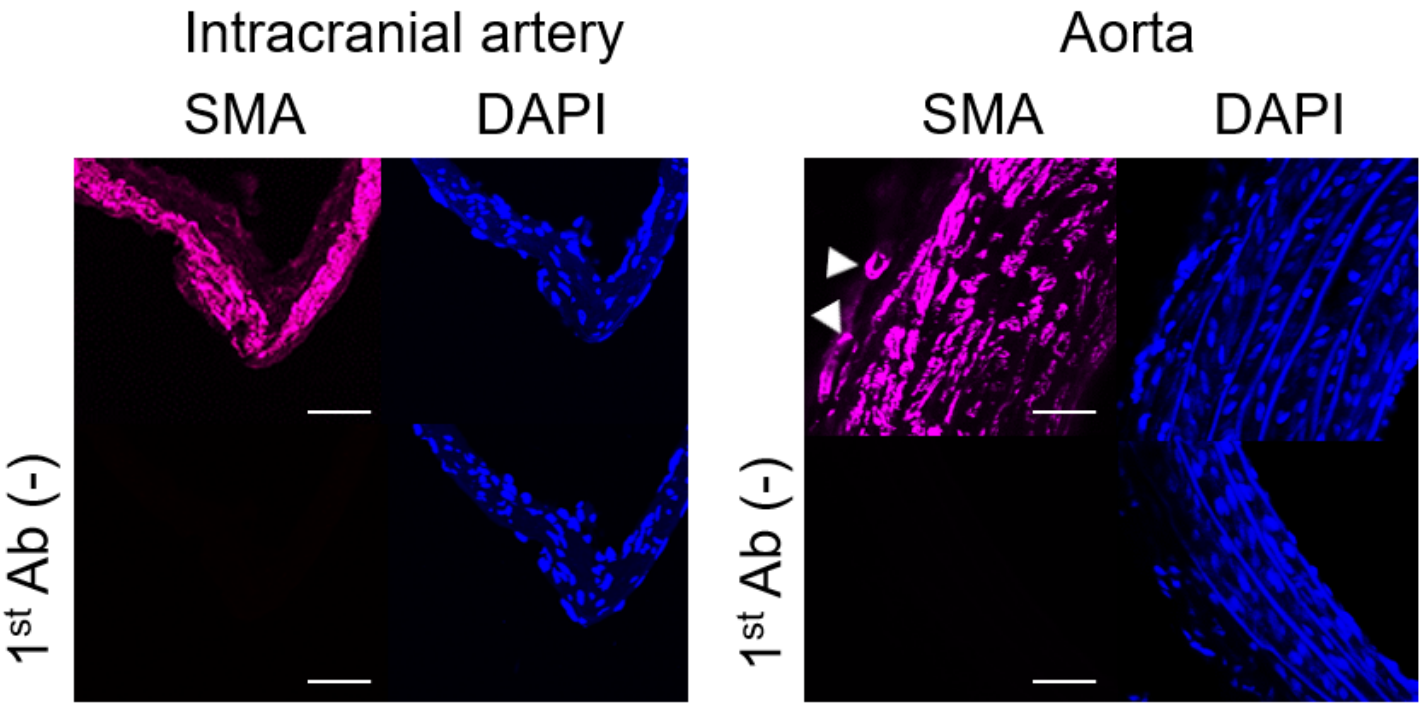

Figure 1

The absence of vasa vasorum in intracranial arteries

The images of immunofluorescent staining of intracranial arteries (left panels) or aorta (right panels) for the marker for smooth muscle cell, a-smooth muscle actin (SMA, red) and nuclear staining by DAPI (blue) are shown. Arrows indicate the vasa vasorum at the adventitia. Scale bar: 50 μm.

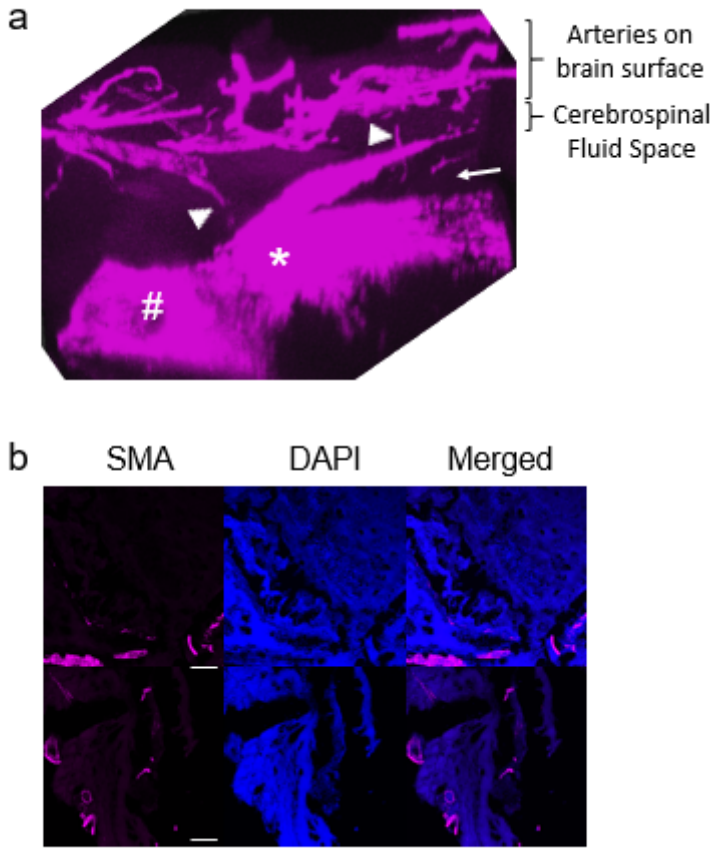

Figure 2

The origin of vasa vasorum migrating into the adventitia of intracranial aneurysmal lesions

Vasa vasorum running from arteries on brain surface. Intracranial aneurysm (IA) lesions and the surrounding structure were visualized by immunohistochemistry for medial smooth muscle cells with tissue transparency. The images of immunofluorescent staining of IA lesions for the marker for smooth muscle cell, a-smooth muscle actin (SMA, red), nuclear staining by DAPI (blue in b), and merged images (b) are shown. The images in (b) are from slices to confirm the presence of vasa vasorum in IA lesions. Scale bar: 50 μm. Arrowhead; arteries from the brain surface, Arrow; the point of rupture, *; dome of the IA, #; the parent artery.

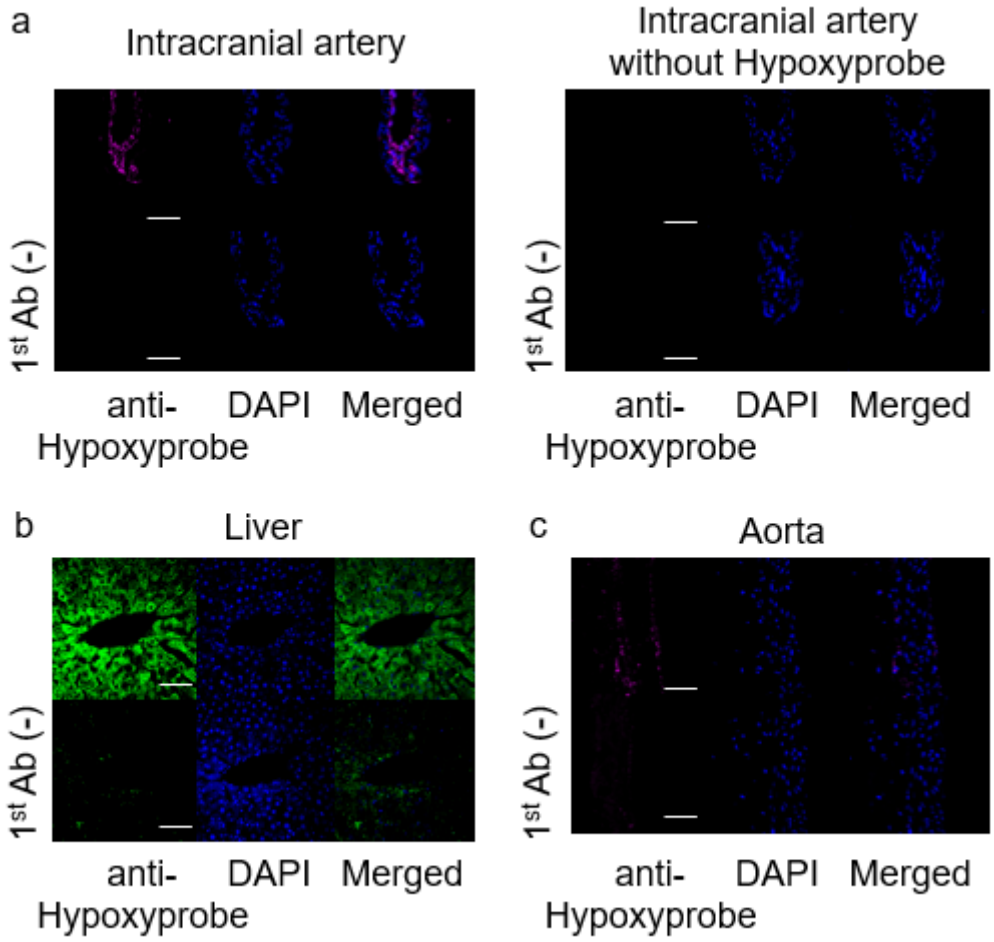

Figure 3

Presence of hypoxic microenvironment in the adventitia of intracranial arterial walls

Hypoxyprobe, the derivative of Pimonidazole, was administered to rats (60 mg/kg) to label hypoxic cells or tissues and the presence of this probe in intracranial arterial walls was detected in immunohistochemistry using the specific antibody. The images of immunofluorescent staining of intracranial arterial walls (a), liver served as a positive control (b) or aorta (c) for Hypoxyprobe (red in a and c, green in b), nuclear staining by DAPI (blue), and merged images are shown. The images from immunohistochemistry without a primary antibody or ones from specimens without the administration of Hypoxyprobe were served as a negative control. Scale bar: 50 μm.

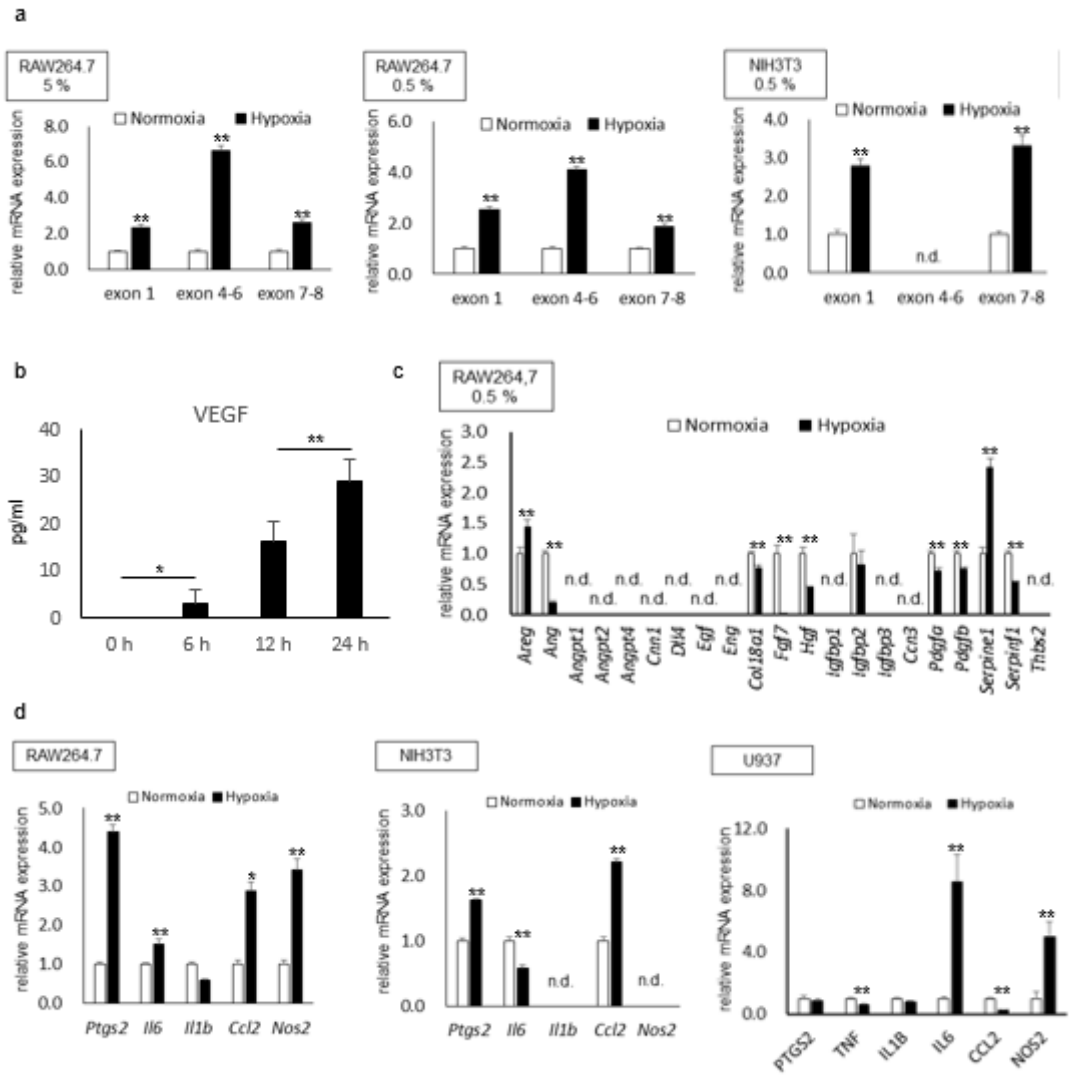

Figure 4

Induction of VEGF and pro-inflammatory factors in cultured cells *in vitro*

Induction of VEGF (a, b), angiogenic factors (c) or pro-inflammatory factors (d) in cultured cells *in vitro*. RAW264.7 cells, NIH3T3 cells or U937 cells were cultured in hypoxic condition (5 % or 0.5 %) for 8 h (a, c, d) or indicated time period (b). The induction of *Vegf* (a), angiogenic factors (c) or pro-inflammatory factors (d) was then examined by RT-PCR analyses (a, c, d, n=6) and the secretion of VEGF by ELISA (b, n=6). Data represents as Mean and S.E.M. Statistical analysis was done by a non-parametric Mann-Whitney test or by a Kruskal-Wallis test followed by a Steel test. *: $p<0.05$, **: $p<0.01$.

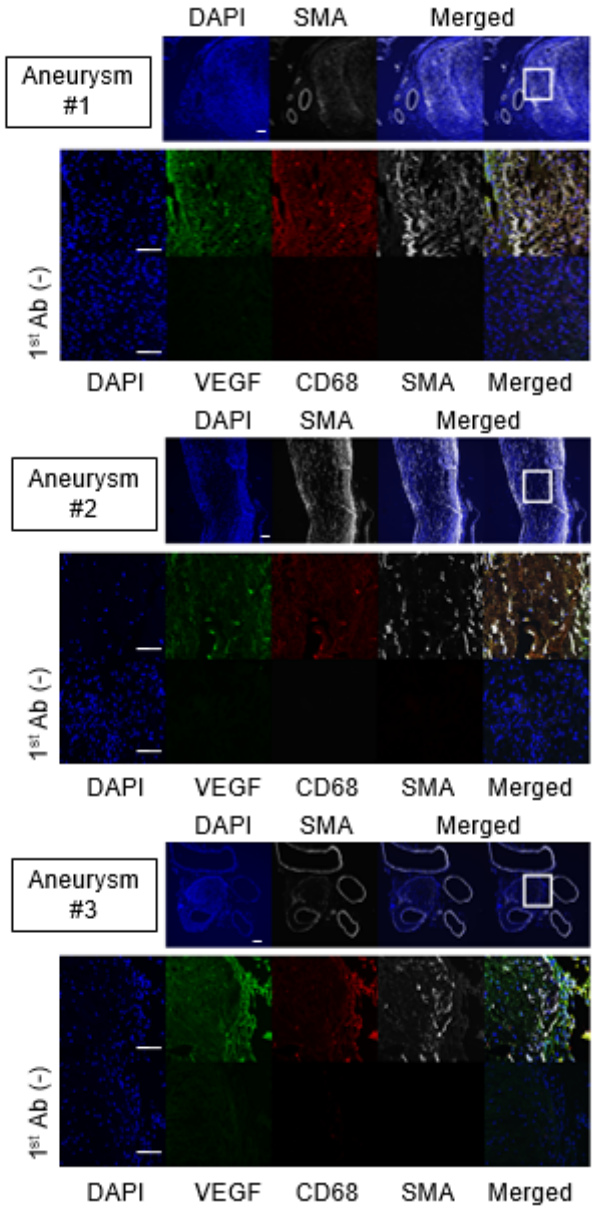

Figure 5

Expression of VEGF in intracranial aneurysm lesions induced in rats.

Expression of VEGF in rupture-prone intracranial aneurysm (IA) lesions induced in rats. The images of immunofluorescent staining of IA lesions for VEGF (green), the marker for macrophages, CD68 (red), the marker for smooth muscle cell, a-smooth muscle actin (SMA, gray), nuclear staining by DAPI (blue), and merged images are shown. The images from immunohistochemistry without a primary antibody were served as a negative control. Magnified images corresponding to the square in the upper panels are shown in the lower panels. Scale bar: 50 μm.

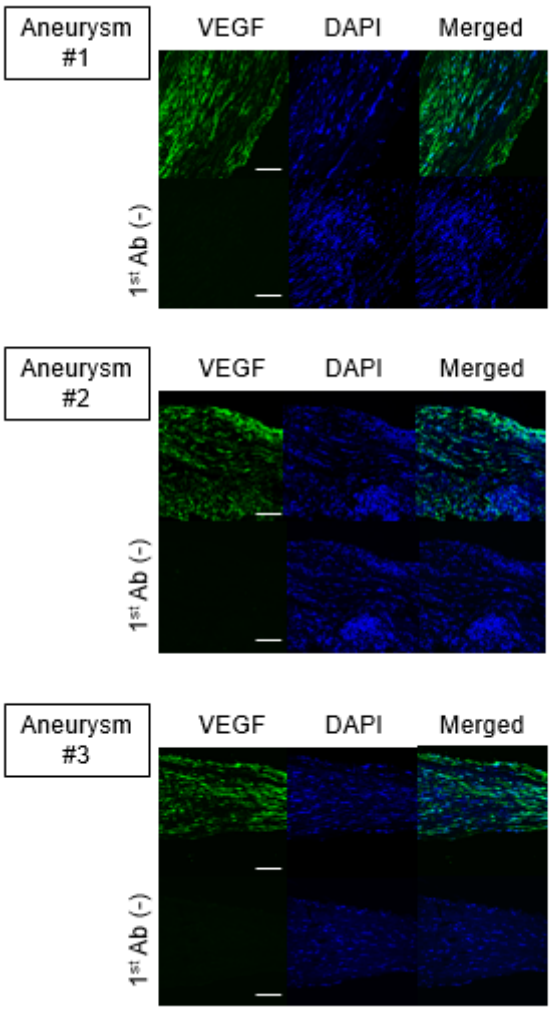

Figure 6

Expression of VEGF in human intracranial aneurysm lesions

Expression of VEGF in human unruptured intracranial aneurysm (IA) lesions. The images of immunofluorescent staining of IA lesions for VEGF (green), nuclear staining by DAPI (blue), and merged images are shown. The images from immunohistochemistry without a primary antibody were served as a negative control. Scale bar: 50 μm.

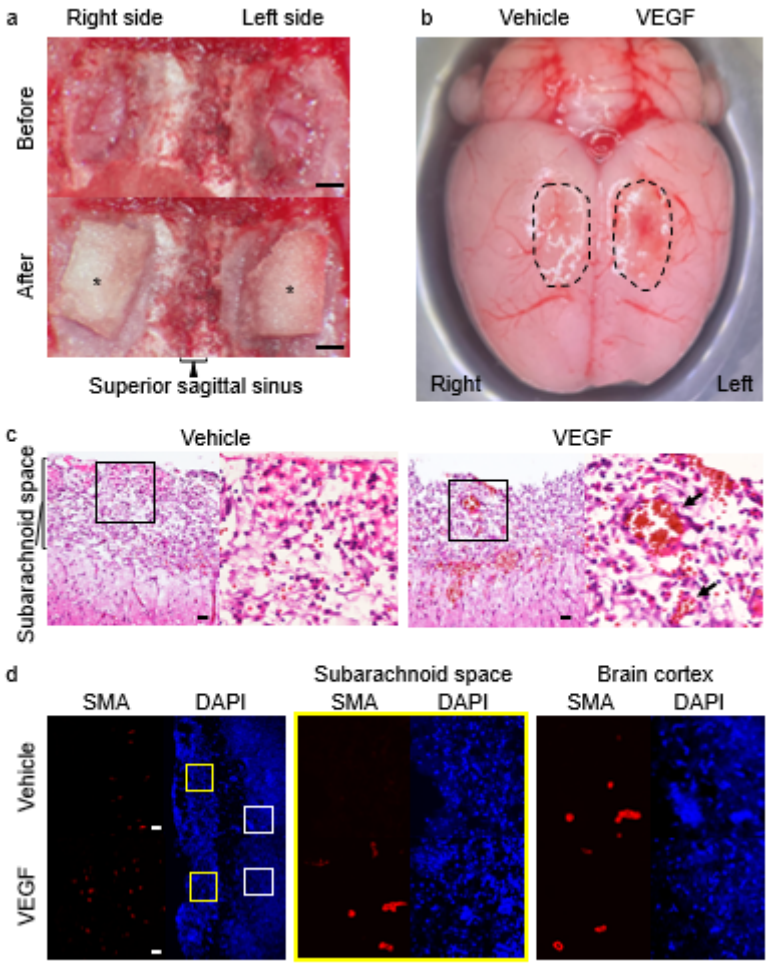

Figure 7

VEGF-mediated induction of neovessels in subarachnoid space

The sheet for slow-release of VEGF or vehicle was placed on the right or the left of brain surface in the same rat (a) and the induction of vasa vasorum in subarachnoid space was examined. Asterisks indicate the sheets placed on brain surface. Scale bar: 1 mm. The macroscopic image of the brain surface (b) and the histopathological images from Hematoxylin-Eosin staining from specimen of vehicle- or VEGF-treated side (c) are shown. Dotted circles in (b) indicate the region where the sheet was placed. Noted the reddish appearance only in the VEGF-treated side indicating the induction of neovessels. Magnified images corresponding to the square in the left panels in (c) are shown on the right. Arrows indicate the neovessels induced in subarachnoid space. Scale bar: 50 μm. The images of immunofluorescent staining for the marker for smooth muscle cell, a-smooth muscle actin (SMA, red), nuclear staining by DAPI (blue), and merged images are shown. Magnified images corresponding to the squares in the left panels are shown on the right. Scale bar: 100 μm.